Rafael Kenji Nishihora, Mara Gabriela Novy Quadri, Dachamir Hotza, Kurosch Rezwan, Michaela Wilhelm

Tape casting of polysiloxane-derived ceramic with controlled porosity and surface properties

Rafael Kenji Nishihora, Mara Gabriela Novy Quadri, Dachamir Hotza, Kurosch Rezwan, Michaela Wilhelm,
Tape casting of polysiloxane-derived ceramic with controlled porosity and surface properties,
Journal of the European Ceramic Society, Volume 38, Issue 15, 2018, Pages 4899-4905, ISSN 0955-2219,
https://doi.org/10.1016/j.jeurceramsoc.2018.07.016

Original Article

Tape casting of polysiloxane-derived ceramic with controlled porosity and surface properties

Rafael Kenji Nishihora[a,b], Mara Gabriela Novy Quadri[b], Dachamir Hotza[b], Kurosch Rezwan[a,c], Michaela Wilhelm[a,*]

[a] University of Bremen, Advanced Ceramics, Am Biologischen Garten 2, IW3, D-28359 Bremen, Germany
[b] Department of Chemical Engineering and Food Engineering (EQA), Federal University of Santa Catarina (UFSC), 88040-900, Florianópolis, SC, Brazil
[c] MAPEX Center for Materials and Processes, University of Bremen, 28359 Bremen, Germany

ARTICLE INFO

Keywords:
Polymer-derived ceramics (PDCs)
Polysiloxanes
Tape casting
Sacrificial pore former
Silicon oxycarbide (SiOC)

ABSTRACT

Tape casting has been applied to produce porous hybrid and SiOC ceramic tapes using ceramic precursors and commercially available polysiloxanes as polymeric binders. SiC particles of two different mean sizes (4.5 or 6.5 μm) were used as inert fillers to prevent shrinkage and increase mechanical stability. Macroporosity was adjusted by varying the azodicarbonamide (ADA) content from 0 to 30 wt.%. Decomposition of the polysiloxanes at 600 °C resulted in the generation of micropores with high specific surface area (187–267 $m^2 g^{-1}$) and a predominant hydrophobic behavior. At 1000 °C mainly meso/macroporosity were observed (SSA: 32–162 $m^2 g^{-1}$) accompanied by increased hydrophilicity. The influence of ADA content, SiC size, and pyrolysis temperature on open porosity (2.5–37%), average pore size (< 0.01–1.76 μm), surface characteristics, and flexural strength (10.5–121 MPa) were investigated. The porous tapes with different surface characteristics and controlled structure are highly promising for applications involving membrane processes, particularly microfiltration systems (0.1–10 μm).

1. Introduction

Tape casting is a well-established wet shaping process at industrial and laboratory scales. Conventionally, a tape casting slurry is composed of a solvent, organic polymers as binders and plasticizers, surfactants, and ceramic particles which are left after burning out the organic compounds [1,2]. This technique is traditionally applied to produce planar thin ceramic tapes (10–1000 μm) for electronic components such as dense multilayered substrates [3].

The advances in ceramic processing and the increasing interest in developing porous ceramic materials allowed the fabrication of thin ceramic tapes for a wide range of applications, such as: solid oxide fuel cells [4–6], photocatalysis [7], supports/substrates [8–10], and microfiltration [11,12]. There are plenty of strategies to produce macroporous ceramic tapes which include sacrificial pore formers, freeze casting, phase-inversion, and partial sintering [13].

However, depending on the application, a hierarchical structure with micro-meso-macropores may be required. Macropores (> 50 nm) are responsible for providing mechanical stability and improved mass transport, while micro (< 2 nm) and mesopores (2–50 nm) have a major influence on the functional properties and specific surface area (SSA) [14]. To this end, the incorporation of micro-mesopores and functional properties is feasible by using preceramic polymers (PCPs) such as polysiloxanes. PCPs are capable of undergoing different shaping processing routes due to their polymeric nature [15–17]. Furthermore, these precursors can be converted into hybrid ceramics (at 500–700 °C) [18], when parts of the polymers remain unreacted. When ceramic materials (SiC, SiOC, SiCN) are formed from silicon-based polymers by heat treatment (≥1000 °C) under inert atmospheres [19], those products are described as polymer-derived ceramics (PDCs).

Sacrificial templating, direct foaming, freeze casting, emulsion based or etching methods have been applied to shape porous polymer-derived ceramics [20,21]. Most of those studies are mainly focused on the production of bulk systems like monolithic or foam structures. Therefore, there are only a few mentions in the literature regarding the use of polysiloxanes as polymeric binder for the tape casting process [10,22,23]. Ceramic tapes from silanes/polysiloxanes have been fabricated using PCPs as binders and ceramic precursors, eventually including SiC as inert filler to avoid shrinkage, and Si as active filler to generate pores [10,22]. After pyrolysis at high temperatures (1200–1600 °C) under inert atmosphere (Ar or N_2), a Si-O-C-(N) ceramic system was obtained. Nevertheless, to the best of our

* Corresponding author.
E-mail address: mwilhelm@uni-bremen.de (M. Wilhelm).

knowledge, the capability of producing tape casted hybrid ceramic was not investigated.

Polysiloxanes may result in hybrid ceramics with high specific surface area, due to the formation of micropores, when pyrolyzed below 700 °C [18], keeping the hydrophobic character of the polymers. On the other hand, pyrolysis at higher temperatures (≥1000 °C) leads to a collapse of micropores and a hydrophilic behavior is developed due to the decomposition and ceramization process [24]. Macroporosity can be produced by adding sacrificial pore formers like azodicarbonamide (ADA) [25,26].

Therefore, the present study focuses on the processability of polysiloxanes to produce PCP-based tapes with adjustable porosity and surface properties in terms of hydrophilicity or hydrophobicity.

2. Material and methods

2.1. Precursors, solvent and additives

All experiments were performed using commercially available chemicals with no additional purification step. Powders of methylphenyl polysiloxane (Silres® H44, Wacker Chemie) and methyl polysiloxane (Silres® MK, Wacker Chemie) were used as binders and ceramic precursors. Silicon carbide powders (SiC F800, d_{50} = 6.5 μm; and SiC F1000, d_{50} = 4.5 μm; EKS) were used as inert fillers to increase processability, reduce cracking due to shrinkage, and provide mechanical stability after pyrolysis. Azodicarbonamide (ADA, 97%, CAS 123-77-3, Sigma–Aldrich) was used as pore former. Imidazole (99%, A10221, CAS 288-32-4, Alfa Aesar) was applied as a cross-linking catalyst for the polysiloxanes. Xylene (98.5%, CAS 1330-20-7, Sigma–Aldrich) was the solvent for the polysiloxanes and the liquid medium to disperse the other components.

2.2. Preparation of the polysiloxane-based tapes

The preparation procedure of the polysiloxane-based tapes is shown in Fig. 1. The first step comprises the slurry preparation, which was conducted at room temperature (r.t.) using magnetic stirrer. Firstly, MK (20 wt.%) and H44 (20 wt.%) powders were dissolved in xylene to get a clear solution. SiC (59 wt.%; d_{50} = 4.5 or 6.5 μm) was then added into the obtained solution and stirred for 60 min to produce a homogeneous slurry. Finally cross-linking catalyst, imidazole (1 wt.%) was added and stirred for further 60 min. In order to understand the effect of ADA, this pore former agent was added in various amounts. It was added in the obtained clear solution of MK and H44 before the addition of SiC. The calculation of the ADA (0, 10, 20, and 30 wt.%) was based on the total weight of the other solid components in the composition (MK + H44 + SiC + imidazole = 100 wt.%). The slurry was casted over a polyethylene terephthalate carrier film (Mylar, G10JRM, Richard E. Mistler, Inc.) using a doctor blade with the gap set at 1.5 mm. The tape was dried at room temperature in a fume hood for 24 h prior to cutting. Afterward, the cut pieces were dried for at least more 24 h before pyrolysis. The tapes were pyrolyzed at 600 and 1000 °C in an atmosphere of nitrogen. The heating rate was 120 °C h^{-1} to 100 °C below the final temperature and 30 °C h^{-1} to the final temperature with a dwelling time of 4 h. The overall appearance of the pyrolyzed tapes at 600 and 1000 °C is shown in Fig. 1.

2.3. Sample notation

Tapes were composed by varying the particle size of SiC and the weight percentage of ADA regarding the total amount of the other solids in the slurry. Sample notation was based on the following construction: SiCX –AY–Z, where X means the silicon carbide average particle size in μm; A stands for ADA; Y refers to the ADA weight percentage (wt.%); and Z is the pyrolysis temperature in °C.

2.4. Characterization

The macrostructure was analyzed by Scanning Electron Microscopy (SEM, 20 kV; Series 2, Obducat CamScan). For this purpose, the samples were sputtered with gold (K550, Emitech, Judges Scientific). The surface roughness (Ra) was determined in triplicate with an optical profilometer (Pll2300, Sensofar). Porosity and mean pore size of the tapes were determined using mercury intrusion porosimetry (Pascal 140/440, Porotec). Specific BET surface area (SSA) was determined by nitrogen adsorption and desorption isotherms measured at 77 K (Belsorp-Mini, Bel Japan). The samples were degassed at 120 °C for 3 h. Before degassing, the pyrolyzed tapes were ground and sieved with a 300 μm mesh sieve in order to diminish the limitation of nitrogen diffusion within the timeframe of the experiment. Hydrophilicity and

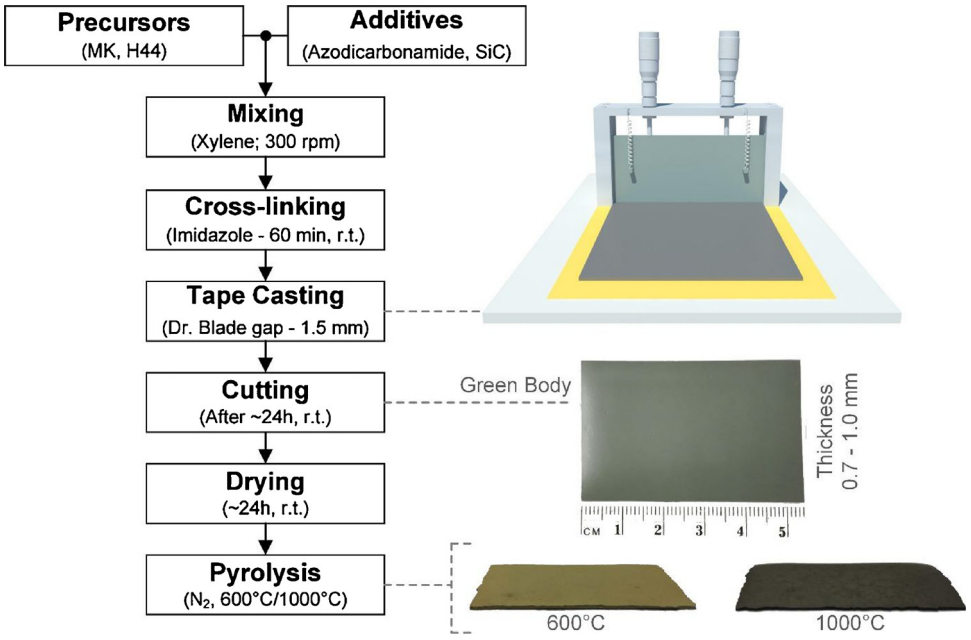

Fig. 1. Flowchart of polysiloxane-derived, casted and pyrolyzed tapes (600/1000 °C).

hydrophobicity were studied by water and n-heptane vapor adsorption measurements, which were carried out by placing vessels with ~0.4 g of sample powder (particle sizes ≤ 300 μm) inside closed Erlenmeyer flasks filled with the solvent at equilibrium with its vapor phase at room temperature (~22 °C). Samples were weighted at the start and end of a 24 h measurement period in order to determine the vapor uptake of the material. Later, the uptake was recalculated into g m^{-2} using the specific surface area of the materials.

The maximum flexural strength (σ_{max}) of the pyrolyzed tapes was obtained by three-point bending tests (Roell Z005, Zwick – DIN EN 843-1 [27]). These measurements were performed using a 5 kN load cell (piezoelectric force sensor). The samples were cut in a rectangular shape (16 mm length, ~2 mm width, and 0.7–1.0 mm thickness) and placed in the center of a sample holder with 10 mm distance between the support rollers (diameter of 1.5 mm). The crosshead speed and preload were fixed at 0.1 mm min^{-1} and 0.25 N, respectively. Ten samples for each composition and temperature were tested and statistically evaluated by analysis of variance (ANOVA) with Tukey's test at a significance level of $p < 0.05$.

3. Results

Preparation of hybrid ceramic and ceramic tapes was performed by using polysiloxanes as precursors, which feature methyl and/or phenyl groups. The green bodies were stable and easy to handle. To prevent excessive bending of the tapes during pyrolysis, porous ceramic weights were placed on the samples. The final pyrolyzed tapes show different colors owing to the pyrolysis temperature (see Fig. 1). At 600 °C, hybrid ceramic (brownish sample) is produced whilst at 1000 °C (black sample) the methyl and phenyl groups are decomposed resulting in the amorphous SiOC ceramic [28]. All pyrolyzed samples possessed sufficient handling stability. The pore forming agent content and SiC particle size were varied to investigate their influence on pore structure and mechanical properties.

3.1. Pore morphology and macroporosity

The pore morphology originated by adding ADA was investigated by SEM. Considering that the resultant structures for all samples with ADA are quite similar, one composition was selected to be shown in this work. The pyrolyzed tapes (600 and 1000 °C) produced with 30 wt.% ADA and the SiC with two mean particle sizes (d_{50} = 4.5 or 6.5 μm) is shown in Fig. 2. Most of the pores exhibit an irregular spheroidal shape that seems to be homogeneously distributed in the matrix. The macroporous structures depicted by SEM evidence pores slightly smaller than 1 μm up to around 7 μm. Regarding the surface roughness (Ra, Fig. S1), it was observed a slight increment of Ra by increasing SiC size and pyrolysis temperature for samples without ADA. Samples containing ADA presented a stiff increase of Ra compared to samples without ADA. This could be related to the higher viscosity observed in the slurry due to the addition of ADA, which possibly causes the enlargement of the surface roughness during casting. However, after pyrolysis at both temperatures (600 °C/1000 °C), ADA did not show any positive correlation on surface roughness. On the contrary, samples with 30 wt.% of ADA exhibited a slight decrease in Ra after pyrolysis. This response is probably a result of the facilitated gas releasing from the polysiloxane matrix due to the pores originated from ADA decomposition, which prevents further alteration of the surface.

It is worth mentioning that ADA is normally used as a physical blowing agent in non-cross-linked PCPs, which results in foam structures with large macropores (0.1–1.5 mm) [25,29]. In this work, ADA was entrapped by the cross-linked polysiloxanes, so that the typical foaming process could not take place. From the images no distinguishable differences in morphology concerning pyrolysis temperatures and inert filler sizes is observable. In addition, SiC particles seem to be embedded by the pre-ceramic polymer. Nevertheless, samples produced with larger SiC particles appear to have some inner defects that resemble cracks (highlighted by the dashed yellow circles in Fig. 2c and d), which can affect the mechanical performance of the tapes.

Fig. 3 presents the results obtained by mercury intrusion porosimetry for all the pyrolyzed tapes. The open porosity varies in the range of 2.5–37% according to the amount of ADA (see Fig. 3a). As expected, an increment on pore former amount leads to increasing open porosity, in this case showing a positive linear relationship. The main factor controlling the open porosity is the ADA content, especially for ADA ≥ 20 wt.%. Despite the fact that adding ADA amounts between 20 and 30 wt.% lead to the highest value of open porosity, the influence of this 10 wt.% increment on the mean pore size is negligible for most samples.

The mean pore diameter (Fig. 3b) can be tailored primarily by altering the inert filler size and pyrolysis temperature. This diameter determined by Hg intrusion represents the interparticle pores in the matrix, which is also called pore window size. The sizes measured are comprehended between < 0.01–1.76 μm. SiC4.5 samples exhibit a minor increase in the pore diameter due to the rising temperature. However, SiC6.5 samples are greatly affected by pyrolysis temperature. The increment of the average pore size for the SiC6.5–1000 °C samples (0.89–1.76 μm) was around 3 times the value detected for SiC6.5–600 °C samples (< 0.01–0.63 μm). The SiC4.5-A30 samples presented a bimodal pore size distribution (see Fig. S2), which can indicate the collapse of a small volume of the small pores. For all other pyrolyzed tapes, a monomodal distribution was observed, although the pore window size distribution was broadened for the sample SiC6.5-A30-1000 °C.

3.2. Surface area and surface characteristics

The N_2 adsorption-desorption isotherms and specific surface areas (SSA) of the pyrolyzed tapes were investigated in order to determine the influence that pyrolysis temperature and tape composition (ADA amount and SiC size) may play on the microstructure. Fig. 4a displays the specific surface area obtained from the nitrogen adsorption isotherms (see Fig. S3). Specific surface areas up to 267 $m^2 g^{-1}$ were obtained for tapes pyrolyzed at 600 °C without azodicarbonamide, which are reduced to around 187 $m^2 g^{-1}$ (SiC4.5-A30-600 °C) due to the addition of 30 wt.% pore former. The reduction of the specific surface area is more noticeable by increasing the temperature rather than the pore former content. The increment of azodicarbonamide resulted in a slight linear decrease of SSA, which is expected due to the introduction of macroporosity in the structure. Inert filler size does not show any significant effect on the specific surface area of samples pyrolyzed at 600 °C.

On the other hand, for the samples pyrolyzed at 1000 °C, the particle size showed some considerable impact on SSA. Samples with smaller particle size (4.5 μm) result in a higher SSA at 1000 °C. For the SiC4.5–1000 °C specimens with pore former amount of 0 to 30 wt.%, SSA decrease from 162 to 77 $m^2 g^{-1}$, respectively. Conversely, samples with 6.5 μm SiC particles (SiC6.5–1000 °C) varied in the range of 76 $m^2 g^{-1}$ (SiC6.5-A0-1000 °C) to 32 $m^2 g^{-1}$ (SiC6.5-A30-1000 °C). Comparable values were reported in the literature for monoliths produced via aqueous freeze casting using pyrolyzed H44 (600 °C) as filler [30].

The nitrogen sorption isotherms of the samples pyrolyzed at 600 °C can be classified as a type I isotherm (Fig. 4b or all the isotherms see Fig. S3). This is typical for microporous solids (< 2 nm) where the limiting uptake is governed by the accessible micropore volume rather than by the internal surface area [31]. The shape of isotherms for samples pyrolyzed at 1000 °C, especially those with 4.5 μm SiC particles, are associated with type IV isotherm, which is common for mesoporous (2–50 nm) materials, where capillary condensation takes place. A very small hysteresis loop is shown in these isotherms, which corresponds to a hysteresis loop type H4. This type of loop is often

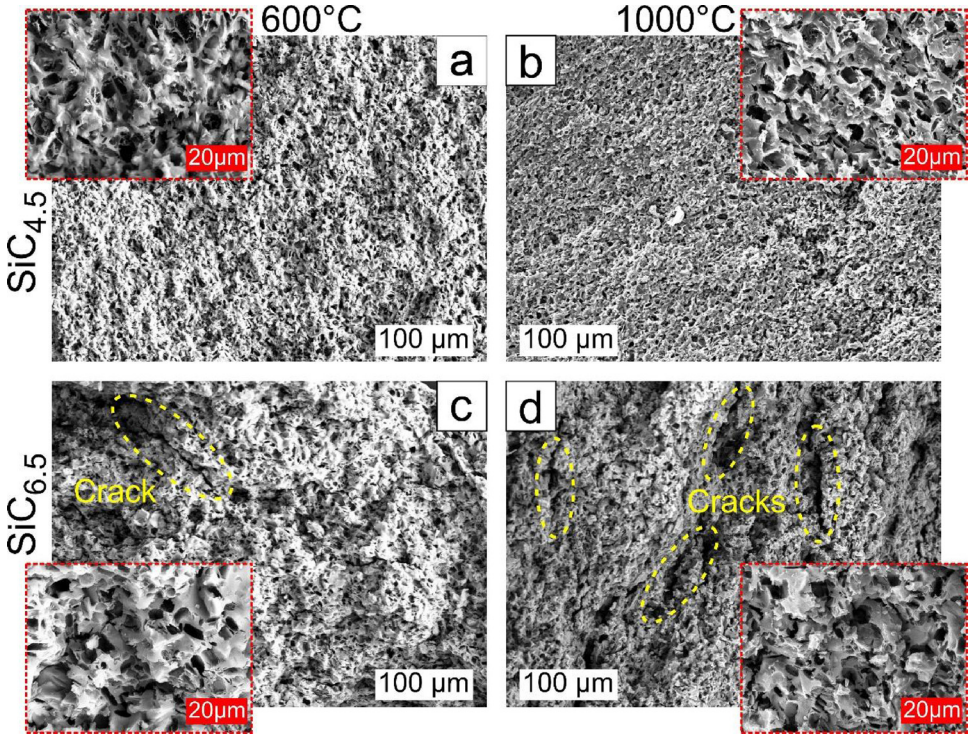

Fig. 2. SEM images from the fracture of the pyrolyzed tapes at 600 or 1000 °C and 30 wt.% pore former (azodicarbonamide): (a) SiC4.5-A30-600 °C, (b) SiC4.5-A30-1000 °C, (c) SiC6.5-A30-600 °C, (d) SiC6.5-A30-1000 °C. Horizontal length of the white and red boxes represents the sizes given therein (For interpretation of the references to color in this figure legend, the reader is referred to the web version of this article).

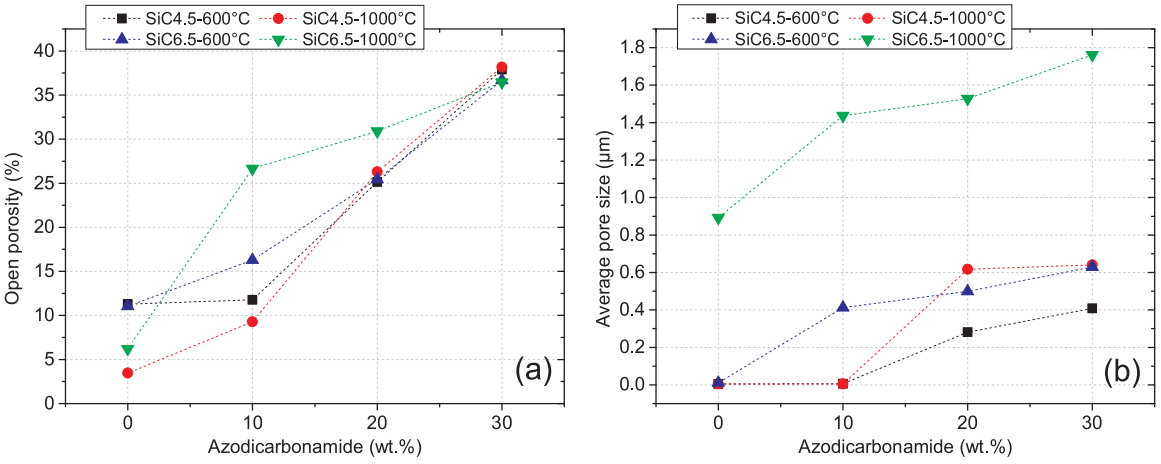

Fig. 3. Influence of ADA content on open porosity (a) and average pore size (b).

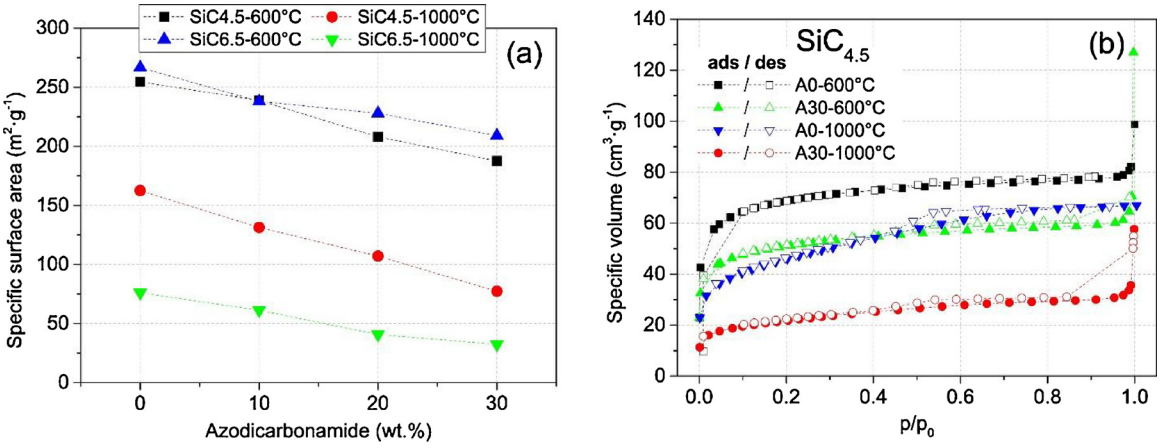

Fig. 4. (a) Influence of ADA content and different SiC particle sizes (4.5 or 6.5 μm) on specific BET surface areas of pyrolyzed (600/1000 °C) tapes, (b) Isotherms obtained for two tape compositions ($SiC_{4.5}$-A0 and A30) pyrolyzed at 600 °C and 1000 °C.

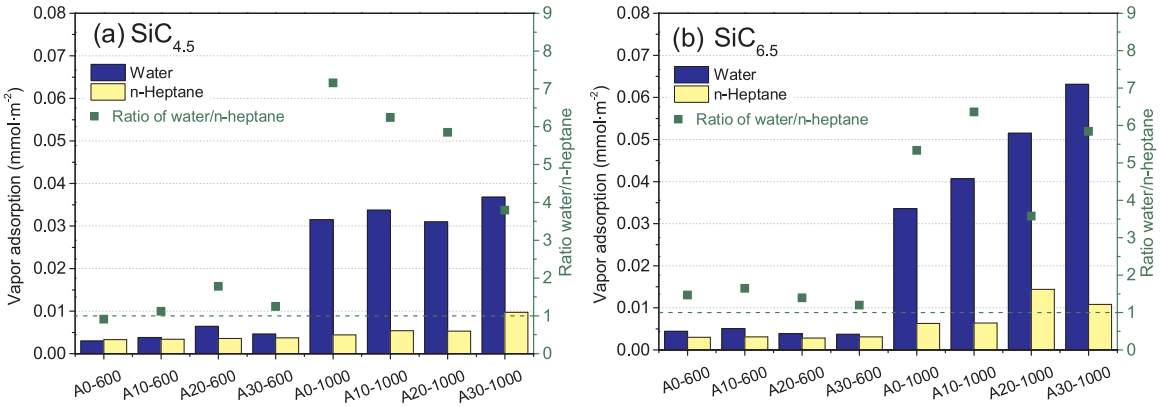

Fig. 5. Water and n-heptane vapor adsorption at ~22 °C (left axis) and ratio of maximum water and n-heptane adsorption (right axis) for samples with different SiC particle size of 4.5 μm (a) and 6.5 μm (b), varying azodicarbonamide amount and pyrolysis temperature (600 and 1000 °C).

associated with narrow slit-like pores [31].

Considering that water contact angle method is quite sensitive to surface heterogeneity and presence of porosity, the vapor adsorption of polar (water) and non-polar (n-heptane) solvents was adopted to describe the surface behavior. Hydrophilicity and hydrophobicity characteristics of the pyrolyzed tapes are displayed in Fig. 5. Apparently, there is no influence of SiC size and ADA amount on the vapor adsorption because this property is a particular feature of the pyrolyzed polysiloxanes. Hence, the surface characteristic is dictated by the pyrolysis temperature. Beyond 600 °C, most of the remaining hydrophobic methyl groups of the preceramic polymer are decomposed, resulting in higher hydrophilicity [28,32]. Despite the fact that most of the samples present hydrophilic nature in terms of water-to-heptane ratio (> 1), tapes pyrolyzed at 600 °C clearly tend to be more hydrophobic (1 ≤ ratio ≤ 2) than those pyrolyzed at 1000 °C (3.5 < ratio < 7.5). For instance, the average amount of water vapor adsorbed by tapes produced at 600 °C increased from 0.0044 ± 0.0010 mmol m^{-2} to 0.0402 ± 0.0114 mmol m^{-2} after pyrolysis at 1000 °C, which represents an increment of 9.2 times. In contrast, the increase of the adsorption of n-heptane is only about 2.4 times, from 0.0033 ± 0.0003 mmol m^{-2} to 0.0078 ± 0.0035 mmol m^{-2}.

3.3. Flexural strength of the pyrolyzed tapes

The maximum flexural strength (σ_{max}) of the pyrolyzed tapes was measured using three-point bending test. Fig. 6 depicts the σ_{max} (MPa) for all tape compositions as a function of the azodicarbonamide amount. The highest strength could be achieved at 1000 °C when using smaller inert filler without pore former addition (121 ± 15 MPa). However, increasing the amount of ADA leads to a lowering of the mechanical strength since mechanical stability is compromised by the introduction of pores/porosity [33]. Apparently, the decrease of σ_{max} according to the increment of ADA exhibited an exponential pattern. The lowest values observed for σ_{max} were 18.9 ± 2.8 MPa (SiC4.5-A30-600 °C), 15.9 ± 3.1 MPa (SiC6.5-A20-600 °C), 10.5 ± 3.6 MPa (SiC6.5-A30-600 °C).

In order to evaluate the statistical differences in the flexural strength data, two sets of analysis were performed using ANOVA with Tukey's test at a significance level of $p < 0.05$ (Fig. 6). Fig. 6 describes the difference due to ADA addition at a fixed SiC size and temperature by analyzing the columns (same color), where the samples statistically different are indicated by letters with their respective color. Because of the exponential decay trend is possible to see that most of the samples were statistically different when low ADA content was used (0–10 wt.%). In this regard, the average flexural strength was very similar for higher amount of ADA (≥ 20 wt.%), where just the samples SiC4.5-A20-1000 °C – SiC4.5-A30-1000 °C and SiC6.5-A20-600 °C – SiC6.5-A30-600 °C seems to be statistically different. In those samples

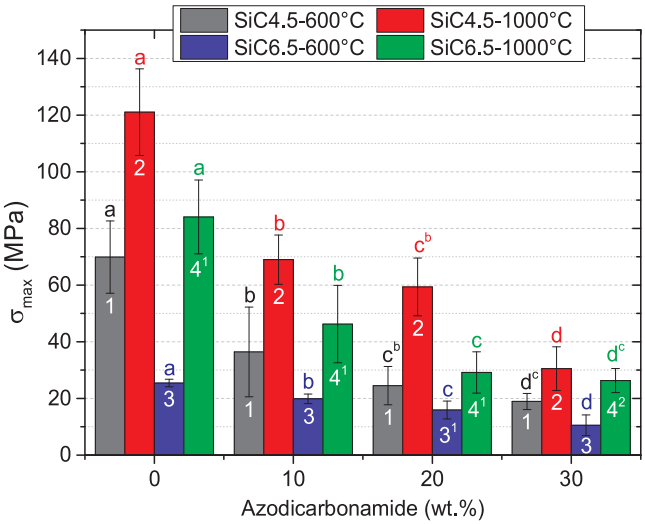

Fig. 6. Maximum flexural strength (σ_{max}) of the tapes produced with two silicon carbide particle sizes, pyrolyzed at 600/1000 °C and varying pore former content. (Values with the same amount of ADA followed by different numbers were significantly different at $p < 0.05$ according to Tukey's test – Columns with the same color followed by different letters were significantly different at $p < 0.05$ according to Tukey's test.).

(SiC6.5–600 °C) a linear decay can be implied.

Analyzing Fig. 6 by looking at the numbers placed inside the columns it is possible to see the difference due to the SiC particle size and temperature at a fixed ADA content. Most of the samples differ statistically from each other, and the strongest tapes are obtained at 1000 °C using an inert filler with 4.5 μm and 6.5 μm, respectively. Interestingly, the specimens SiC4.5–600 °C (column 1) and SiC6.5–1000 °C (column 4) between 0 and 20 wt.% ADA content are not statistically different. This indicates the great influence of the inert filler size on the mechanical stability of porous materials. Meanwhile, at the highest ADA content (30 wt.%) only the samples pyrolyzed at 1000 °C do not differ statistically, which implies that at this point there is no influence of the SiC size on flexural strength. However, there is a difference when comparing the samples SiC4.5-A30-600 °C and SiC6.5-A30-600 °C, which indicates the positive influence of SiC size at 600 °C.

4. Discussion

The use of a liquid shaping process as tape casting was feasible with polysiloxanes acting as a binder, which after heating under controlled atmosphere resulted in a hybrid polymer/ceramic matrix. The incorporation of macroporosity in the structure was achieved by using

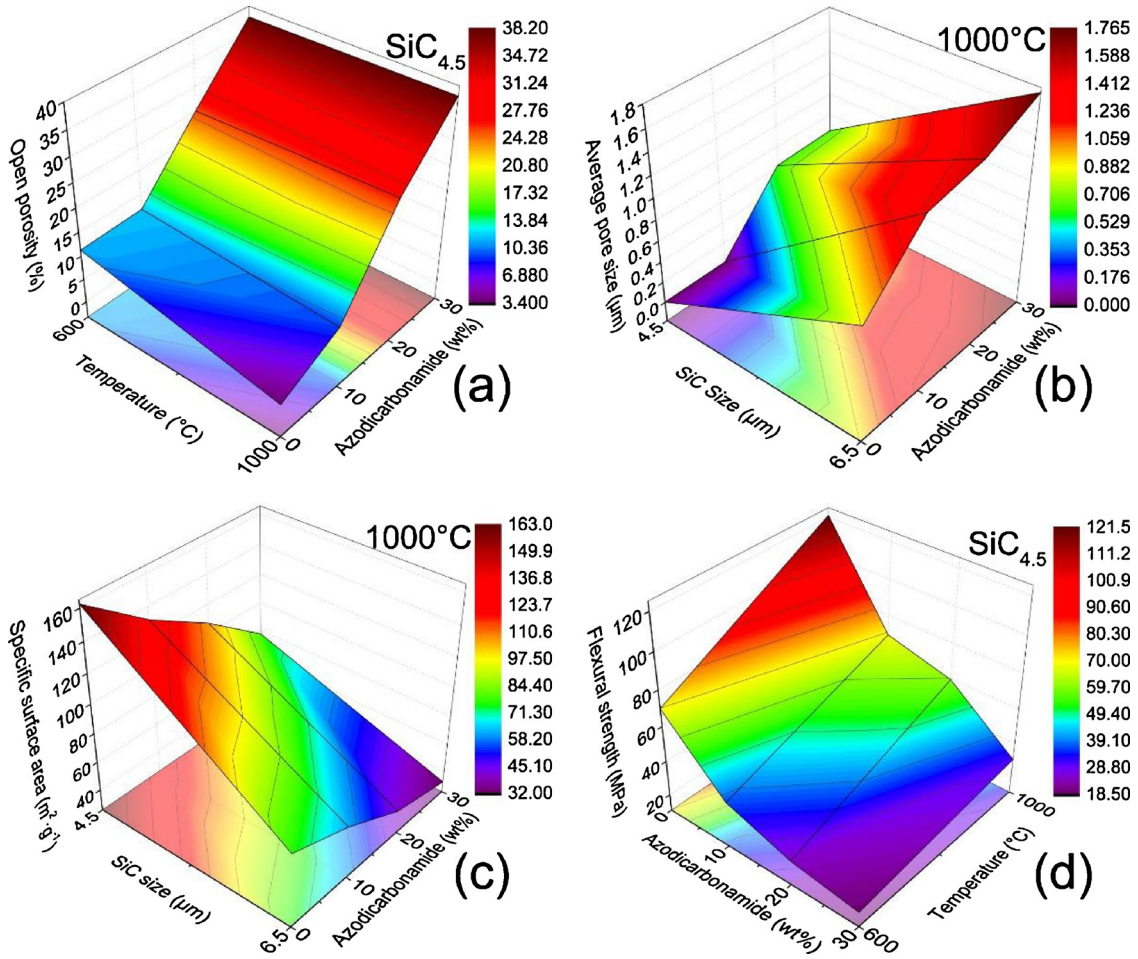

Fig. 7. 3D representation of the influence of azodicarbonamide amount, pyrolysis temperatures, and inert particle size on: open porosity (a); average pore size (b); specific surface area (c); and maximum flexural strength (d).

ADA as pore former agent. The 3D representation in Fig. 7a shows that the main parameter responsible for creating open macroporous is the addition of ADA, especially for amounts larger than 10 wt.%. Within the 20–30 wt.% range, the macroporosity and open pore size are greatly amplified. On the other hand, the shape of the surface in Fig. 7b indicates the additional influence of the inert filler size on the average pore size. The increase in the pore size is more noticeable using 6.5 μm SiC particles pyrolyzed at 1000 °C. This response is presumably due to larger vacancies between particle-to-particle contacts. Thus, after burning at 1000 °C small pores completely collapsed into bigger ones, which was not the case for SiC4.5.

In contrast, microporosity is negatively affected by the insertion of macroporosity and high pyrolysis temperature. Fig. 7c demonstrates that at 1000 °C inert filler size plays a major role in sustaining larger SSA. Probably the use of microsized inert filler combined with the slow heating rate can hinder the complete collapse of micro/mesopores in the material [34]. This assumption may be sustained by the occurrence of isotherms type IV with hysteresis loop H4 in all the samples pyrolyzed at 1000 °C (see Fig. S2), particularly when using smaller inert filler (4.5 μm). Thus, some of the micropores formed due to the thermal decomposition of the cross-linked polymer collapsed into mesopores, which maintained a substantial value of SSA even after pyrolysis at 1000 °C [24].

Considering that the inert fillers are embedded in the polysiloxane matrix, the hydrophobic/hydrophilic behavior is tailored by the preceramic polymer and its thermal treatment. The tendency toward a hydrophobic behavior can be observed at temperatures below 600 °C since the organic groups, such as methyl and phenyl, are not completely decomposed. Furthermore, the hydrophobicity may also be increased by using a higher amount of MK [18] because the decomposition of methyl groups requires more energy as compared to phenyl groups [35]. Nonetheless, hydrophilicity is achieved by applying high temperatures (≥1000 °C) where ceramization takes place [36], modifying polysiloxanes with hydrophilic cross-linking agents (e.g. APTES) [24], or increasing the relative amount of a specific polymer (e.g. H44) [18].

Mechanical stability of porous ceramics is directly related to their microstructure, porosity, type and size of particles (inert filler in this case), bonding, etc. Fig. 7d shows the major influence of temperature and porosity (azodicarbonamide content) on the maximum flexural strength of the tape. Increment in porosity means enlarging macrodefects in the structure, which drastically reduced the σ_{max} in both studied temperatures (600 and 1000 °C). Regarding temperature, at 1000 °C high mechanical strength is expected due to ceramization process. Another factor that may enhance the σ_{max} at high pyrolysis temperature is the presence of free carbon between the Si—O—C bonds [37,38]. Moreover, the use of smaller inert filler also contributed to improving σ_{max} (see Fig. 6), which is probably connected to the higher number of particle-to-particle contacts. The lower mechanical performance of porous SiC6.5 samples can also be correlated to the internal cracks identified in the SEM pictures (Fig. 2c and d).

5. Conclusions

Polysiloxane-based ceramics with hierarchical pore structure were produced by tape casting. Open macroporosity was controlled by using azodicarbonamide as a sacrificial pore former. Since ADA was

entrapped in the cross-linked polysiloxanes matrix, its foaming behavior was suppressed. Pyrolysis at 600 °C generated microporosity in the structure, consequently, a higher SSA was obtained. Furthermore, a hydrophobic behavior is more pronounced at 600 °C whereas at 1000 °C hydrophilicity is increased as observed by vapor adsorption analysis. At 1000 °C, micropores collapsed into meso-macropores mostly. Although mechanical stability could be increased by using smaller inert filler and higher pyrolysis temperature, the introduction of macroporosity drastically diminished the flexural strength. The average pore size can be controlled mainly by the inert filler size and pyrolysis temperature. The range of values combined with the tailored surface characteristics indicated a potential application of this material for membrane separation processes such as microfiltration systems (0.1–10 μm).

Acknowledgements

The Deutsche Forschungsgemeinschaft (DFG) as well as the Brazilian funding agencies National Council for Scientific and Technological Development (CNPq) and Coordination for the Improvement of Higher Education Personnel (CAPES) through the Brazilian-German Collaborative Research Initiative on Manufacturing (BRAGECRIM) are gratefully acknowledged. The authors would like also to thank the support of the Erasmus + programme of the European Union for the academic exchange between the University of Bremen and the Federal University of Santa Catarina.

Appendix A. Supplementary data

Supplementary material related to this article can be found, in the online version, at doi:https://doi.org/10.1016/j.jeurceramsoc.2018.07.016.

References

[1] R.E. Mistler, The principles of tape casting and tape casting applications, in: R.A. Terpstra, P.P.A.C. Pex, A.H. de Vries (Eds.), Ceram. Process. Springer, Netherlands, Dordrecht, 1995, pp. 147–173, , https://doi.org/10.1007/978-94-011-0531-6_5.
[2] D. Hotza, P. Greil, Review: aqueous tape casting of ceramic powders, Mater. Sci. Eng. A 202 (1995) 206–217, https://doi.org/10.1016/0921-5093(95)09785-6.
[3] R.E. Mistler, E.R. Twiname, Tape Casting: Theory and Practice, Wiley, 2000.
[4] M. Boaro, J.M. Vohs, R.J. Gorte, Synthesis of highly porous Yttria-stabilized Zirconia by tape-casting methods, J. Am. Ceram. Soc. 86 (2003) 395–400, https://doi.org/10.1111/j.1151-2916.2003.tb03311.x.
[5] S. Ramanathan, K.P. Krishnakumar, P.K. De, S. Banerjee, Powder dispersion and aqueous tape casting of YSZ-NiO composite, J. Mater. Sci. 39 (2004) 3339–3344, https://doi.org/10.1023/b:jmsc.0000026934.88520.67.
[6] H. Moon, S.D. Kim, S.H. Hyun, H.S. Kim, Development of IT-SOFC unit cells with anode-supported thin electrolytes via tape casting and co-firing, Int. J. Hydrogen Energy 33 (2008) 1758–1768, https://doi.org/10.1016/j.ijhydene.2007.12.062.
[7] L. Ren, Y.-P. Zeng, D. Jiang, The improved photocatalytic properties of P-type NiO loaded porous TiO_2 sheets prepared via freeze tape-casting, Solid State Sci. 12 (2010) 138–143, https://doi.org/10.1016/j.solidstatesciences.2009.09.021.
[8] W.A. Meulenberg, J. Mertens, M. Bram, H.-P. Buchkremer, D. Stöver, Graded porous TiO_2 membranes for microfiltration, J. Eur. Ceram. Soc. 26 (2006) 449–454, https://doi.org/10.1016/j.jeurceramsoc.2005.06.035.
[9] A. Sanson, P. Pinasco, E. Roncari, Influence of pore formers on slurry composition and microstructure of tape cast supporting anodes for SOFCs, J. Eur. Ceram. Soc. 28 (2008) 1221–1226, https://doi.org/10.1016/j.jeurceramsoc.2007.10.001.
[10] F. Scheffler, M. Scheffler, Polymer derived ceramic tapes as substrate and support for zeolites, Adv. Appl. Ceram. 108 (2009) 468–475, https://doi.org/10.1179/174367609X459540.
[11] N. Das, S. Bandyopadhyay, D. Chattopadhyay, H.S. Maiti, Tape-cast ceramic membranes for microfiltration application, J. Mater. Sci. 31 (1996) 5221–5225, https://doi.org/10.1007/bf00355928.
[12] N. Das, H.S. Maiti, Formatation of pore structure in tape-cast alumina membranes – effects of binder content and firing temperature, J. Memb. Sci. 140 (1998) 205–212, https://doi.org/10.1016/S0376-7388(97)00282-2.
[13] R.K. Nishihora, P.L. Rachadel, M.G.N. Quadri, D. Hotza, Manufacturing porous ceramic materials by tape casting-a review, J. Eur. Ceram. Soc. 38 (2018) 988–1001, https://doi.org/10.1016/j.jeurceramsoc.2017.11.047.
[14] P. Colombo, C. Vakifahmetoglu, S. Costacurta, Fabrication of ceramic components with hierarchical porosity, J. Mater. Sci. 45 (2010) 5425–5455, https://doi.org/10.1007/s10853-010-4708-9.
[15] P. Greil, Polymer derived engineering ceramics, Adv. Eng. Mater. 2 (2000) 339–348, https://doi.org/10.1002/1527-2648(200006)2:6<339::AID-ADEM339>3.0.CO;2-K.
[16] G. Mera, E. Ionescu, Silicon-containing preceramic polymers, Encycl. Polym. Sci. Technol. John Wiley & Sons, Inc., 2002, https://doi.org/10.1002/0471440264.pst591.
[17] E. Ionescu, Polymer-derived ceramics, Ceram. Sci. Technol. Wiley-VCH Verlag GmbH & Co. KGaA, 2012, pp. 457–500, https://doi.org/10.1002/9783527631957.ch18.
[18] T. Prenzel, M. Wilhelm, K. Rezwan, Pyrolyzed polysiloxane membranes with tailorable hydrophobicity, porosity and high specific surface area, Microporous Mesoporous Mater. 169 (2013) 160–167, https://doi.org/10.1016/j.micromeso.2012.10.014.
[19] P. Colombo, G. Mera, R. Riedel, G.D. Sorarù, Polymer-derived ceramics: 40 years of research and innovation in advanced ceramics, J. Am. Ceram. Soc. 93 (2010) 1805–1837, https://doi.org/10.1111/j.1551-2916.2010.03876.x.
[20] B.V. Manoj Kumar, Y.-W. Kim, Processing of polysiloxane-derived porous ceramics: a review, Sci. Technol. Adv. Mater. 11 (2010) 44303, https://doi.org/10.1088/1468-6996/11/4/044303.
[21] C. Vakifahmetoglu, D. Zeydanli, P. Colombo, Porous polymer derived ceramics, Mater. Sci. Eng. R Rep. 106 (2016) 1–30, https://doi.org/10.1016/j.mser.2016.05.001.
[22] P. Cromme, M. Scheffler, P. Greil, Ceramic tapes from preceramic polymers, Adv. Eng. Mater. 4 (2002) 873–877, https://doi.org/10.1002/1527-2648(20021105)4:11<873::AID-ADEM873>3.0.CO;2-G.
[23] J.-F. Drillet, M. Adam, S. Barg, A. Herter, D. Koch, V. Schmidt, M. Wilhelm, Development of a novel zinc/air fuel cell with a Zn foam anode, a PVA/KOH membrane and a MnO_2/SiOC-based air cathode, ECS Trans. 28 (2010) 13–24, https://doi.org/10.1149/1.3507923.
[24] H. Zhang, C.L. Fidelis, A.L.T. Serva, M. Wilhelm, K. Rezwan, Water-based freeze casting: adjusting hydrophobic polymethylsiloxane for obtaining hierarchically ordered porous SiOC, J. Am. Ceram. Soc. 100 (2017) 1907–1918, https://doi.org/10.1111/jace.14782.
[25] A. Idesaki, P. Colombo, Synthesis of a Ni-containing porous SiOC material from polyphenylmethylsiloxane by a direct foaming technique, Adv. Eng. Mater. 14 (2012) 1116–1122, https://doi.org/10.1002/adem.201100354.
[26] M. Adam, C. Vakifahmetoglu, P. Colombo, M. Wilhelm, G. Grathwohl, Polysiloxane-derived ceramics containing nanowires with catalytically active tips, J. Am. Ceram. Soc. 97 (2014) 959–966, https://doi.org/10.1111/jace.12708.
[27] DIN EN 843-1, Advanced technical ceramics - mechanical properties of monolithic ceramics at room temperature - part 1: determination of flexural strength, Beuth (2006) p. 24.
[28] M. Naviroj, S.M. Miller, P. Colombo, K.T. Faber, Directionally aligned macroporous SiOC via freeze casting of preceramic polymers, J. Eur. Ceram. Soc. 35 (2015) 2225–2232, https://doi.org/10.1016/j.jeurceramsoc.2015.02.013.
[29] M. Fukushima, P. Colombo, Silicon carbide-based foams from direct blowing of polycarbosilane, J. Eur. Ceram. Soc. 32 (2012) 503–510, https://doi.org/10.1016/j.jeurceramsoc.2011.09.009.
[30] H. Zhang, P. D'Angelo Nunes, M. Wilhelm, K. Rezwan, Hierarchically ordered micro/meso/macroporous polymer-derived ceramic monoliths fabricated by freeze-casting, J. Eur. Ceram. Soc. 36 (2016) 51–58, https://doi.org/10.1016/j.jeurceramsoc.2015.09.018.
[31] K.S.W. Sing, D.H. Everett, R.A.W. Haul, L. Moscou, R.A. Pierotti, J. Rouquerol, T. Siemieniewska, Reporting physisorption data for gas/solid systems with special reference to the determination of surface area and porosity (Recommendations 1984), Pure Appl. Chem. 57 (1985) 603–619, https://doi.org/10.1351/pac198557040603.
[32] T. Prenzel, K. Döge, R.P.O. Motta, M. Wilhelm, K. Rezwan, Controlled hierarchical porosity of hybrid ceramics by leaching water soluble templates and pyrolysis, J. Eur. Ceram. Soc. 34 (2014) 1501–1509, https://doi.org/10.1016/j.jeurceramsoc.2013.11.033.
[33] J.B. Wachtman, W.R. Cannon, M.J. Matthewson, Mechanical Properties of Ceramics, John Wiley & Sons, Ltd., 2009.
[34] H. Schmidt, D. Koch, G. Grathwohl, P. Colombo, Micro- / macroporous ceramics from preceramic precursors, J. Am. Ceram. Soc. 55 (2001) 2252–2255, https://doi.org/10.1111/j.1151-2916.2001.tb00997.x.
[35] P. Olier, L. Delchet, S. Breunig, Tailoring new silicone oil for aluminum demolding, Organosilicon Chem. I From Mol. to Mater. WILEY-VCH Verlag GmbH, 2008, pp. 687–769, https://doi.org/10.1002/9783527620777.ch5be.
[36] M. Scheffler, T. Gambaryan-Roisman, T. Takahashi, J. Kaschta, H. Muenstedt, P. Buhler, P. Greil, Pyrolytic decomposition of preceramic organo polysiloxanes, Ceram. Trans. 115 (2000) 239–250 https://www.tib.eu/de/suchen/id/BLCP%3ACN042344424/Pyrolytic-Decomposition-of-Preceramic-Organo-Polysiloxanes/.
[37] H.J. Kleebe, Y.D. Blum, SiOC ceramic with high excess free carbon, J. Eur. Ceram. Soc. 28 (2008) 1037–1042, https://doi.org/10.1016/j.jeurceramsoc.2007.09.024.
[38] G. Puyoo, G. Chollon, R. Pailler, F. Teyssandier, Microstructure and thermodynamic descriptions of SiC-based ceramic fibers, Mech. Prop. Perform. Eng. Ceram. Compos. V, John Wiley & Sons, Inc., 2010, pp. 159–172, https://doi.org/10.1002/9780470944127.ch17.